

Tailoring coercivity and magnetic anisotropy of Co nanowire arrays by microstructure

Yong Ren · Jianbo Wang · Qingfang Liu ·
Yingying Dai · Bin Zhang · Longgang Yan

Received: 5 December 2010 / Accepted: 17 June 2011 / Published online: 1 July 2011
© Springer Science+Business Media, LLC 2011

Abstract To tailor coercivity and magnetic anisotropy, we have fabricated Co nanowire arrays in the pores of anodic aluminum oxide templates by electrodeposition. Microstructure measurements performed by X-ray diffraction show that Co nanowire arrays are hexagonal close-packed (HCP) structures with different crystalline textures. A wide range in change of coercivity from 925 to 3310 Oe at 300 K, with a maximum of up to 4050 Oe at 5 K, can be found for nanowire arrays with a diameter of 20 nm. This may be the highest value and the widest range of coercivity reported for Co nanowires prepared by electrodeposition method. This finding could be attributed to the adjustment of the microstructure of the cobalt nanowire arrays prepared in different experimental conditions. We have also investigated the relationship between the crystalline textures and the magnetic properties of Co nanowire arrays using micromagnetic simulation combined with microstructure measurements. The preferred orientation of nanowire arrays, such as (1000) or (0002), is a key factor in determining coercivity. This wide tailoring of coercivity makes possible more promising applications of Co nanowire arrays with fixed diameter and length.

Introduction

Typical magnetic materials (Fe, Co, and Ni), such as zero-dimensional nanoparticles, one-dimensional nanowires, and two-dimensional nanofilms, have been widely studied because of their importance on fundamental research and technological applications [1–5]. These materials have much wider application fields, which require tunable physical properties, such as in tailoring the structure of magnetic materials to affect their static and dynamic behaviors [6, 7]. After a highly ordered anodic aluminum oxide (AAO) template was fabricated by Masuda and Fukuda [8], various metal nanowire arrays have been prepared using the AAO template method because of its convenience and inexpensiveness [9–14]. Based on the method, AC electrodeposition method has gained more popularity in the synthesis of metal nanowires than DC method because of its simplicity and ease of handling. In the AC method, there are two main factors determining the magnetic properties of nanowire arrays, namely (1) magnetic character of individual nanowire related to its magnetic anisotropy, such as magnetocrystalline anisotropy and shape anisotropy related to the material and the pores of the AAO template and (2) periodicity or symmetry of nanowire arrays related to the magnetostatic interaction among nanowires connected with the interpore distance in the AAO template [15]. Some groups change the magnetic properties of Co nanowires by mainly adjusting length, diameters, and interpore distance of nanowires [16, 17]. Therefore, the magnetic properties of magnetic nanowire arrays with fixed diameters, lengths, and interpore distances are difficult to adjust.

The main origin of magnetic anisotropy in nanowire arrays is shape anisotropy. Magnetocrystalline anisotropy is another natural property of magnetic materials. Among

J. Wang (✉) · Q. Liu · Y. Dai · B. Zhang · L. Yan
Key Laboratory for Magnetism and Magnetic Materials
of the Ministry of Education, Lanzhou University,
Lanzhou 73000, China
e-mail: wangjb@lzu.edu.cn

Y. Ren
State Key Laboratory Cultivation Base for Nonmetal Composites
and Functional Materials, Southwest University of Science and
Technology, Mianyang 621010, China
e-mail: renyong@swust.edu.cn

these nanowire arrays mentioned, Fe and Ni nanowire arrays have huge effective fields of shape anisotropy, which are 10 times more than that of magnetocrystalline anisotropy [1, 18]. For Co nanowire arrays, magnetocrystalline anisotropic constant K_1 of a bulk of HCP Co is $5 \times 10^6 \text{ erg cm}^{-3}$ at room temperature, which almost balances shape anisotropy ($K_s = \pi M_s^2 = 6 \times 10^6 \text{ erg cm}^{-3}$) [19]. In this case, the total magnetic anisotropy of HCP Co nanowire arrays, by adjusting the angle between shape anisotropy and magnetocrystalline anisotropy [20], is possible to control. Generally, increasing the coercivity of HCP Co nanowire arrays, because their magnetocrystalline anisotropy could lower the total effective anisotropy, whose maximum is 2900 Oe as reported [9, 17, 21–23], is a challenge. In this article, we tailored the microstructure and the magnetic properties of Co nanowire arrays with a diameter of 20 nm under different electrodeposition conditions. Coercivity, from 925 to 3310 Oe, was investigated via magnetic measurement. The relationship between structure and magnetic properties of Co nanowire arrays was further studied by micromagnetic simulation combined with experiments.

Experimental

Nanoporous AAO templates were prepared by a two-step anodization process [15, 21]. First, 0.5 mm thick aluminium foils (99.999%) were annealed in a furnace at 500 °C for 5 h to eliminate mechanical stress. The annealed Al foils were degreased and electropolished in a mixed solution of perchloric acid and ethanol. The foils were then anodized in acid solution under constant DC voltage for 1 h. Resultant alumina layers were removed by a mixture of chromic acid and phosphoric acid. Afterward, the foils were anodized again using the same parameters as in the first step. Two electrolytes consisting of 1 M $\text{CoSO}_4 \cdot 7\text{H}_2\text{O}$ and 30 g L^{-1} H_3BO_3 solution or 1 M $\text{Co}(\text{CH}_3\text{COO})_2$ solution were used to prepare Co nanowire arrays. The pH value was adjusted by NaHCO_3 , then electrodeposition was conducted at 200 Hz and 12 V for 5 min. We then prepared five samples called (a) to (e). The experimental details of different samples are listed in Table 1. Similar to sample (c), samples (d) and (e) were annealed at 623 K, and their magnetic measurements were carried out at 300 and 5 K, respectively.

Micromagnetic simulation was used to investigate the micro-magnetic properties of the magnetic nanomaterials [24]. In the present study, three-dimensional (3D) object-oriented micromagnetic framework (OOMMF) was used to study the magnetization reversal processes of single Co nanowire. In 3D OOMMF, the problem was impressed at regular 3D meshes of rectangles with 3D magnetization

spins positioned at the centers of the cells. Evolution of magnetization distribution was obtained by solving the Landau–Lifshitz Ordinary Differential Equation [25],

$$\frac{\partial M(r_i, t)}{\partial t} = -|\bar{\gamma}|M(r_i, t) \times H_{\text{eff}}(r_i, t) - \frac{|\bar{\gamma}|\alpha}{M_s} M(r_i, t) \times [M(r_i, t) \times H_{\text{eff}}(r_i, t)], \quad (1)$$

where $M(r_i, t)$ is the magnetization of the mesh, $H_{\text{eff}}(r_i, t)$ is the effective field of the mesh, $\bar{\gamma}$ is the Landau–Lifshitz gyromagnetic ratio, and α is the damping coefficient.

The effective field is defined as follows:

$$H_{\text{eff}}(r_i, t) = -\frac{1}{\mu_0} \frac{\partial E_{\text{total}}}{\partial M(r_i, t)}, \quad (2)$$

where the average energy density E_{total} is the function of $M(r_i, t)$. In the present study, exchange, self-magnetostatic (demagnetization), anisotropic, and applied field (Zeeman) terms are considered.

$$E_{\text{total}} = E_{\text{exchange}} + E_{\text{demag}} + E_{\text{anisotropy}} + E_{\text{zeeman}}. \quad (3)$$

In the simulation, nanowire diameter was $d = 20 \text{ nm}$, wire length was $L = 2 \mu\text{m}$, and unit cell size was $2.5 \times 2.5 \times 2.5 \text{ nm}^3$, which was approximately the same as the exchange length, $l_{\text{ex}} \propto \sqrt{2A/\mu_0 M_s^2}$. Material parameters used were typical for HCP Co, namely, saturation magnetization $M_s = 1.4 \times 10^6 \text{ A m}^{-1}$, exchange stiffness constant $A = 30 \times 10^{-12} \text{ J m}^{-1}$, and magnetocrystalline anisotropy constant $K = 4.1 \times 10^5 \text{ J m}^{-3}$. The magnetocrystalline easy axis direction was set to parallel and perpendicular to the long axis of nanowire, corresponding with (0002) and (1000) textures, respectively.

Scanning electron microscopy (SEM, Hitachi-S4800, Japan) was used to investigate the morphology of the AAO template. Transmission electron microscope (TEM, Tecnai G² F30) and selected-area electron diffraction (SAED) were used to study the morphology and the structure of cobalt nanowires. Structures of the Co nanowire arrays were studied by X-ray diffraction (XRD, Cu-1.54056 Å, Philips X'pert, Holland). Magnetic properties were measured using a vibrating sample magnetometer (VSM, Lakeshore 7304, USA).

Results and discussion

Magnetic properties of Co nanowire arrays depend on their diameters. In the present study, we chose nanowire arrays with typical diameters of 20 nm. Figure 1 shows the patterns of AAO template and the released Co nanowires. From Fig. 1a and b, the diameters of pores and nanowires were both 20 nm, indicating that the diameter of pores determines the diameter of nanowires. Therefore, a certain diameter of nanowire can be obtained by controlling the

Table 1 The experimental details and main measurement results for the samples of (a), (b), (c), (d), and (e) are presented

Samples	Solution	pH value	Deposition temperature (°C)	Hc and measurement temperature	Texture	K_{eff} ($\times 10^6$ erg/mm ³)
a	CoSO ₄	6.2	60	925 Oe at 300 K	(1000)	2.15
b	CoSO ₄	4.5	20	1885 Oe at 300 K	(1000), (0002), (1010)	3.62
c	Co(ac) ₂	6.3	20	2590 Oe at 300 K	(0002)	4.36
d	Co(ac) ₂	6.3	20	3310 Oe at 300 K	(0002)	6.01
e	Co(ac) ₂	6.3	20	4050 Oe at 5 K	(0002)	

Measurement temperature is corresponding to the magnetic measurement. K_{eff} is the effective anisotropy constant of nanowire arrays

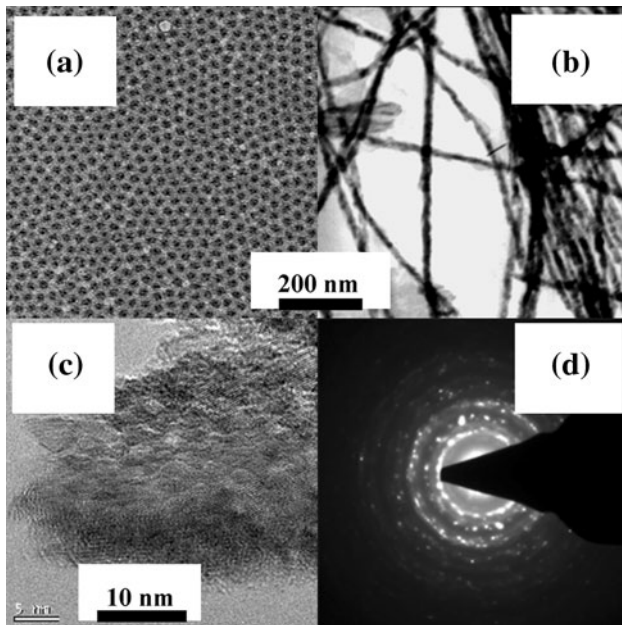


Fig. 1 Typical SEM image of an AAO template (a), TEM image (b), high-resolution TEM picture (c), and SAED pattern (d) of Co nanowire

diameter of pores in the AAO template, which depends on the voltage of oxidation process. High-resolution TEM image and SAED pattern of Co nanowires show that the crystalline grain is polycrystalline in Fig. 1c and d.

Figure 2 shows normalized hysteresis loops of the arrays with 20 nm diameter for samples (a), (b), (c), (d), and (e). The applied field is parallel to the long axis of nanowires, demonstrating that coercivity and remanence ratio (M_r/M_s) continuously increase under different experimental conditions. Minimum and maximum coercivities were 925 and 3310 Oe at 300 K, up to 4050 Oe at 5 K, respectively. These may be the highest values ever reported for Co nanowires prepared by electrodeposition method [9, 17, 22], and the widest adjustment in coercivity with fixed diameter and length. Further, we compared the effective anisotropy constant (K_{eff}) to discuss the total anisotropy of magnetic nanowire arrays and to study the magnetic anisotropy of cobalt nanowire arrays. Figure 3 shows the magnetization curves of samples with different experimental conditions,

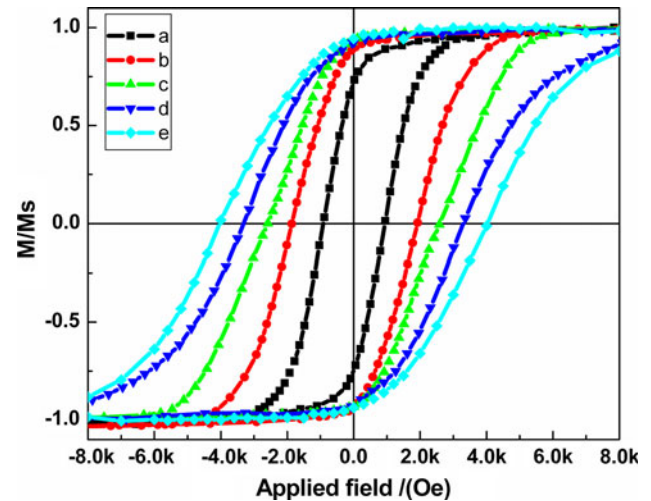


Fig. 2 (Colour online) Normalized hysteresis loops of cobalt nanowire arrays measured with AAO template after removing aluminum corresponding to the sample (a), (b), (c), (d), and (e) with the applied field paralleled to long-axis of wires

and the applied field parallel and perpendicular to the long axis of nanowires. The K_{eff} of nanowire arrays depends on the area between magnetization curves when a magnetic sample is magnetized to saturation. In the present study, K_{eff} was denoted as:

$$K_{\text{eff}} = \frac{M_s}{m_{\text{tot}}} \int_0^{m_{\text{tot}}} H_{\perp} dm - \frac{M_s}{m_{\text{tot}}} \int_0^{m_{\text{tot}}} H_{\parallel} dm, \tag{4}$$

where m_{tot} is the magnetic moment of the sample when magnetized to saturation and H_{\parallel} , H_{\perp} are the applied fields parallel and perpendicular to the long axis of nanowires, respectively [21]. Calculated results of K_{eff} are listed in Table 1. The findings demonstrate that Co nanowire arrays with different textures exhibit different K_{eff} . K_{eff} is lowest for the sample with (1000) texture, but is increased for the sample with peaks of (0002) and (1010), reaching the maximum for the sample with a (0002) texture. The structure of the above-mentioned Co nanowire arrays was investigated to understand the origin of the wide change in coercivity.

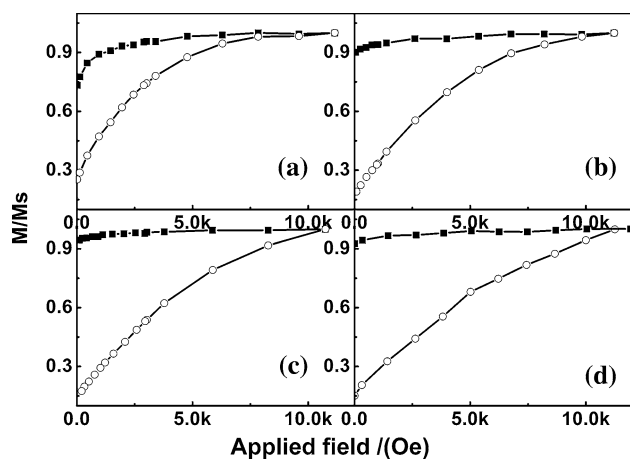


Fig. 3 Magnetization curves for the samples (a), (b), (c), and (d) with the applied field parallel (filled square) and perpendicular (open circle) to the long-axis of nanowire

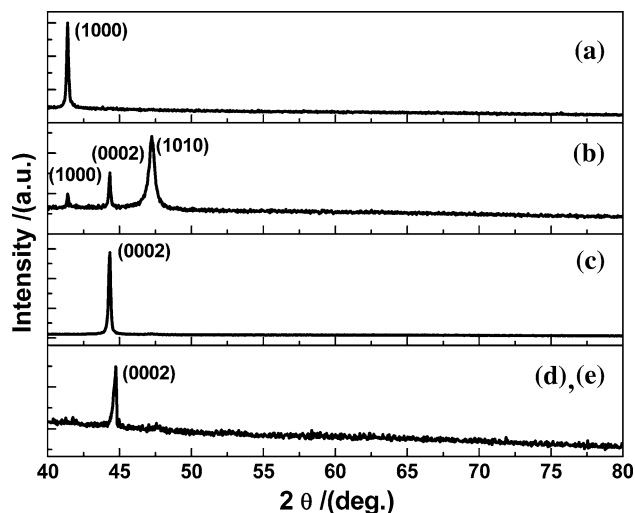


Fig. 4 XRD patterns of sample (a), (b), (c), (d), and (e) measured with AAO template after removing aluminum

Figure 4 shows the XRD results of Co nanowire arrays previously mentioned. The two typical crystal structures of metal cobalt are face-centered cubic (FCC) and HCP phase. These two structures of Co nanowire arrays can be controlled by adjusting the pH value of electrodeposition solution, as discussed by Li and Darques [20, 21, 26]. They indicated that Co nanowire arrays have HCP structures, with a pH of over 3.5. In the present study, the pH value of the electrodeposition solution was higher than 4.5 to obtain pure HCP Co nanowire arrays. Figure 4 shows that the crystal texture of Sample a was (1000). That of Sample b were (1000), (0002), and (1010), whereas that of Sample c was (0002). The XRD results suggest that as-prepared Co should have an HCP structure. Co nanowire arrays with HCP structure show strong magnetocrystalline anisotropy, which is comparable with their shape anisotropy. Further,

HCP Co is a uniaxial magnetocrystalline anisotropy material, and its easy magnetization direction is [0002]. Thus, the different easy magnetization directions of magnetocrystalline anisotropy are results of different crystal textures. Combining XRD results with VSM measurements, nanowire arrays with (1000) texture have the lowest coercivity. Coercivity is enhanced when XRD peaks of (0002) and (1010) appear. The highest coercivity is obtained for the sample with (0002) texture. Micromagnetic simulation is performed to study the static magnetism behavior of the cobalt nanowire, which is helpful in understanding magnetization and magnetization reversal process of nanowires.

Combined with the above analysis, we posited that the texture of (1000) or (0002) plays a key role in influencing the magnetic properties of arrays. Therefore, we simulated two samples with two typical crystalline textures. Figure 5 shows the magnetic hysteresis loops of a single Co nanowire with a diameter of 20 nm and the applied field parallel to the long axis of nanowires via micromagnetic simulation. The figure shows that the coercivity of the (1000) textured nanowire was 1260 Oe, whereas that of the (0002) textured nanowire was 7800 Oe. These findings demonstrated that the coercivity of cobalt nanowire with (0002) texture was much higher than that of the sample with (1000) texture. In the present study, the coercivity of the sample with (0002) texture was more than that of the experimental sample, as only a single Co nanowire was considered at 0 K. Interaction among nanowires and thermal efficiency were neglected. Simulation results also showed the same phenomena compared with the experimental results, which means that the preferred growth orientation of HCP Co nanowires was a crucial factor in influencing the magnetization reversal process. The distributions of static magnetic

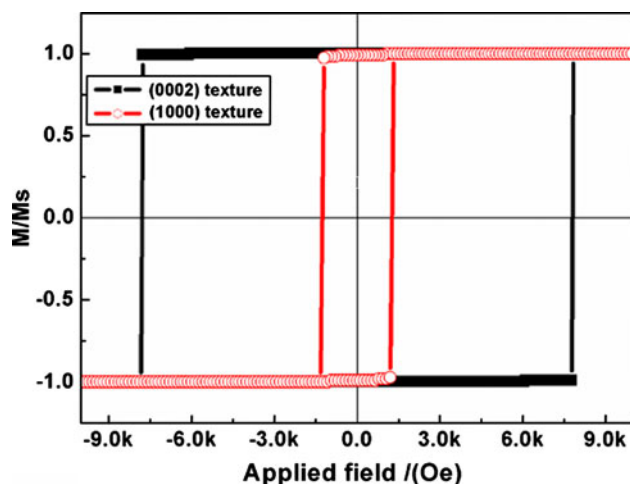


Fig. 5 (Colour online) Normalized hysteresis loops of single cobalt nanowire via micromagnetic simulation corresponding to the sample with (1000) texture (open circle) and (0002) texture (filled square) with the applied field paralleled to long-axis of wires

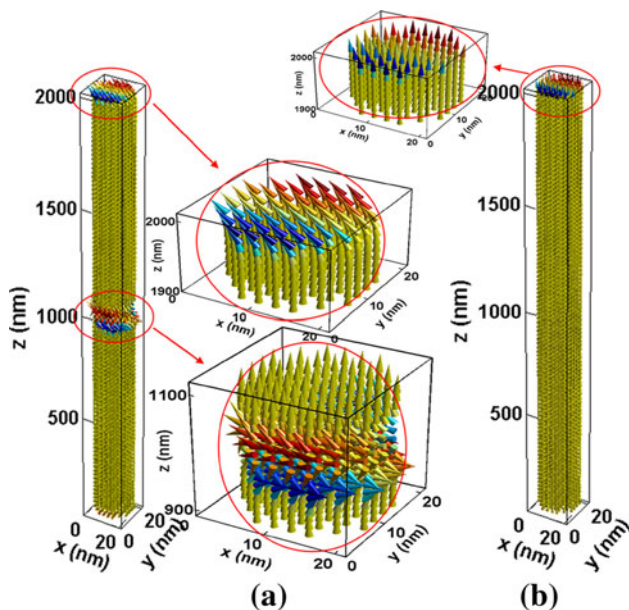


Fig. 6 (Colour online) Distributions of static magnetic moments for the nanowire with texture of (1000) (a) and (0002) (b) simulated via OOMMF

moments with different crystalline textures are shown in Fig. 6. The figure exhibits that almost all magnetic moments of nanowires with (0002) texture were along the long axis of the nanowires (Fig. 6b). However, magnetic vortices appear in the middle of nanowires with (1000) texture (Fig. 6a) as distributions of other magnetic moments are similar to that of nanowires with (0002) texture [27, 28]. It may be concluded that magnetic vortices are related to the crystalline texture (1000). Therefore, the magnetic reversal process of nanowires with (1000) texture is more comparable with that of the sample with (0002) texture. These results can be attributed to the competition between shape anisotropy and magnetocrystalline anisotropy of HCP Co nanowires. This may also be the reason for the wide adjustment of coercivity, from 925 to 3310 Oe at 300 K up to 4050 Oe at 5 K, for the Co nanowire arrays with a diameter of 20 nm.

Conclusion

In summary, we find that the coercivity of Co nanowires with a diameter of 20 nm strongly depends on the preferred orientation of nanowire arrays. Coercivity can be tailored, from 925 to 3310 Oe at 300 K up to 4050 Oe at 5 K, by experimental parameters. This wide adjustment in coercivity leads to more promising application fields for Co nanowire arrays with fixed diameters and lengths. Change in coercivity is related to different K_{eff} aroused by samples

with different textures. Micromagnetic simulation indicates that the angle between the direction of shape anisotropy and the easy magnetization direction of magnetocrystalline anisotropy plays a key role in adjusting the magnetic properties of Co nanowire arrays.

Acknowledgements This work is supported by the NSFC of China (Grant No. 10774061) and Program for New Century Excellent Talents (NCET) in University. Many thanks to the support from Hitachi S-4800 FE-SEM laboratory of Electron Microscope, School of Physical Science and Technology, Lanzhou University. We also acknowledge the support from the CMMM and HPC Center at Lanzhou University.

References

1. Wang JB, Zhou XZ, Liu QF, Xue DS, Li FS, Li B, Kunkel HP, Williams G (2004) *Nanotechnology* 15(5):485
2. Wang CY, Fang JY, He JB, O'Connor CJ (2003) *J Colloid Interface Sci* 259(2):411
3. Xu JX, Wang KY (2008) *Appl Surf Sci* 254(20):6623
4. Chun JY, Lee JW (2010) *Eur J Inorg Chem* 27:4251
5. Xu XJ, Fang XS, Zeng HB, Zhai TY, Bando Y, Golberg D (2010) *Sci Adv Mater* 2(3):273
6. Darques M, Piraux L, Encinas A, Bayle-Guillemaud P, Popa A, Ebels U (2005) *Appl Phys Lett* 86(7):072508
7. Sklyuyev A, Ciureanu M, Akyel C, Ciureanu P, Yelon A (2009) *J Appl Phys* 105(2):023914
8. Masuda H, Fukuda K (1995) *Science* 9:1466
9. Wang PP, Gao LM, Qiu ZY, Song XP, Wang LQ, Yang S, Murakami R (2008) *J Appl Phys* 104(6):064304
10. Ramazani A, Kashi MA, Alikhani M, Erfanfam S (2008) *Mater Chem Phys* 112(1):285
11. Sharma G, Pishko MV, Grimes CA (2007) *J Mater Sci* 42(13):4738. doi:10.1007/s10853-006-0769-1
12. Wu XJ, Zhu F, Mu C, Liang YQ, Xu LF, Chen QW, Chen RZ, Xu DS (2010) *Coord Chem Rev* 254(9–10):1135
13. Yang W, Cui CX, Sun JB, Wang BL (2010) *J Mater Sci* 45(6):1523. doi:10.1007/s10853-009-4116-1
14. Yang JA, Cui CX, Yang W, Hu B, Sun JB (2011) *J Mater Sci* 46(7):2379. doi:10.1007/s10853-010-5085-0
15. Ren Y, Liu QF, Li SL, Wang JB, Han XH (2009) *J Magn Magn Mater* 321(3):226
16. Kartopu G, Yalcin O, Es-Souni M, Basaran AC (2008) *J Appl Phys* 103(9):093915
17. Zeng H, Zheng M, Skomski R, Sellmyer DJ, Liu Y, Menon L, Bandyopadhyay S (2000) *J Appl Phys* 87(9):4718
18. Navas D, Pirota KR, Zelis PM, Velazquez D, Ross CA, Vazquez M (2008) *J Appl Phys* 103(7):07D523
19. Ferre R, Ounadjela K, George JM, Piraux L, Dubois S (1997) *Phys Rev B* 56(21):14066
20. Darques M, Encinas A, Vila L, Piraux L (2004) *J Phys D* 37(10):1411
21. Li FS, Wang T, Ren LY, Sun JR (2004) *J Phys Condens Matter* 16(45):8053
22. Zhang J, Jones GA, Shen TH, Donnelly SE, Li GH (2007) *J Appl Phys* 101(5):054321
23. Maaz K, Karim S, Usman M, Mumtaz A, Liu J, Duan JL, Maqbool M (2010) *Nanoscale Res Lett* 5(7):1111
24. Ren Y, Dai YY, Zhang B, Liu QF, Xue DS, Wang JB (2010) *Nanoscale Res Lett* 5(5):853

25. Donahue MJ, Porter DJ (2002) OOMMF user's guide, version 1.2a3. <http://math.nist.gov/oommf>
26. Darques M, Encinas A, Vila L, Piraux L (2004) *J Phys Condens Matter* 16(22):S2279
27. Ren Y, Wang JB, Liu QF, Zhang B, Han XH, Xue DS (2009) *J Phys D* 42(10):105002
28. Vila L, Darques M, Encinas A, Ebels U, George J-M, Faini G, Thiaville A, Piraux L (2009) *Phys Rev B* 79(17):172410